2006

Experimental Performance of Prototype Carbon Dioxide Compressors

Thomas Christen
Purdue University

Beat Hubacher
Purdue University

Stefan S. Bertsch
Purdue University

Eckhard A. Groll
Purdue University

EXPERIMENTAL PERFORMANCE OF PROTOTYPE CARBON DIOXIDE COMPRESSORS

Thomas CHRISTEN, Beat HUBACHER, Stefan S. BERTSCH*, and Eckhard A. GROLL

Purdue University, Ray W. Herrick Laboratories, School of Mechanical Engineering
West Lafayette, Indiana 47907, USA

*Corresponding Author; Tel: (765 496 2886), Fax: (765 494 0787), E-mail: sbertsch@purdue.edu

ABSTRACT

This paper describes performance measurements of prototype carbon dioxide compressors using a compressor load stand based on a hot-gas bypass design. Five compressors were tested: a semi-hermetic reciprocating single-stage compressor (Type A) with an estimated cooling capacity of 8.3 kW, a hermetic rotary two-stage compressor (Type B) with an estimated cooling capacity of 2.4 kW, a semi-hermetic reciprocating two-stage compressor (Type C) with an estimated cooling capacity of 10.5 kW, a semi-hermetic reciprocating single-stage compressor (Type D) with an estimated cooling capacity of 0.8 kW, and a semi-hermetic reciprocating single-stage compressor (Type E) with an estimated cooling capacity of 1.6 kW.

Compressor tests were conducted for varying suction pressures, superheats and discharge pressures. For each test, refrigerant mass flow rate, power consumption, suction and discharge temperature and pressure were recorded. In addition, the volumetric and overall isentropic efficiencies were calculated. In the end the performance data of all compressors were compared. Volumetric efficiencies range from 0.48 up to 0.90 and the overall isentropic efficiencies range from 0.40 up to 0.71 for pressure ratios between 1.75 and 6.75.

1. INTRODUCTION

The transcritical cycle technology using carbon dioxide as the refrigerant has received increased attention as a possible replacement for the conventional vapor compression cycle technology using fluorocarbon-based refrigerants during the past decade. In particular, four applications of carbon dioxide systems can be identified that show a comparable performance and may be economically feasible compared to vapor compression systems. The most prominent of these applications is automotive air conditioning. By now, most of the major automobile manufacturers possess carbon dioxide prototype systems. The second application is environmental control units (ECU), which are packaged air-to-air air-conditioners that are used in cooling of mission critical electronics and personnel. The third application that shows great promise for transcritical carbon dioxide systems is the one of heat pump water heaters. The fourth application is vending machines and glass door coolers. A detailed review of the latest developments with respect to these applications can be found in Groll (2006).

While the compressor development for automotive air conditioning application has excelled over the last several years, relatively little information is available in the literature with respect to hermetic or semi-hermetic compressors that need to be used in the other three applications mentioned above. Therefore, research was conducted which specifically focused on measuring the performance of carbon dioxide compressors. Details of this study can be found in Hubacher *et al.* (2002) and Hubacher and Groll (2003).

2. BACKGROUND ON CO_2-COMPRESSORS

Most of the early investigations on hermetic-type CO_2 compressors focused on the design issues associated with the use of CO_2 (Fagerli 1996a; Fagerli 1997) or the modification of existing HCFC-22 compressors to use with carbon dioxide (Adolph 1995; Fagerli 1996b; Koehler *et al.* 1997 and 1998; Hwang and Radermacher 1998). In more recent studies, prototype designs of hermetic compressors for use with carbon dioxide have been built and analyzed. Tadano *et al.* (2000) developed a prototype hermetic two-stage rolling piston compressor with a cooling capacity of 750 W. The authors reported isentropic efficiencies of up to 88% not including motor and shell losses. Neksa *et al.*

(2000) reported on the development of a series of semi-hermetic reciprocating compressors (single- and two-stage). A volumetric efficiency of up to 80 % and an isentropic efficiency of up to 60 % were reported for the compressor.

In summary, most investigations with respect to carbon dioxide compressors have focused on developing a prototype compressor or a better understanding of the fundamental concepts of carbon dioxide compression. However, much of the information associated with these studies is not necessarily available to the public and detailed performance data of CO_2 compressors is still difficult to obtain. This information however, is needed to be able to evaluate the performance potential of the transcritical carbon dioxide technology on a system level.

3. CO_2-COMPRESSOR LOAD STAND

For the purpose of measuring the performance of carbon dioxide compressors, a compressor load stand for cooling capacities from 5 to 20 kW was designed and built. The load stand is based on a hot-gas bypass cycle concept as can be seen from the P-h-diagram in *Figure* 1. The key idea behind this concept is to anchor the intermediate pressure below the critical pressure in the two-phase region by condensing a fraction of the refrigerant flow. Using this stable anchoring pressure, the suction and discharge pressures are controlled using appropriate metering valves in the discharge line and bypass line. The compressor discharges supercritical, high pressure, high temperature carbon dioxide, which is throttled to the intermediate pressure equal to the condensation pressure. After passing through the main flow meter the CO_2 flow is split. Most of the flow goes through the bypass loop while the remaining flow enters the primary loop. The bypass loop includes the bypass expansion valve where the fluid is throttled to the suction pressure level. The primary loop condenses the CO_2 in the water-cooled condenser. Subcooled liquid exits the condenser and is throttled through the primary expansion valve to the suction pressure level as well. The two fluid streams are then combined in a straight mixing pipe. A schematic of the load stand indicating all significant features is shown in *Figure 2*. All control valves are based on manual operated valves which allow for very stable operation.

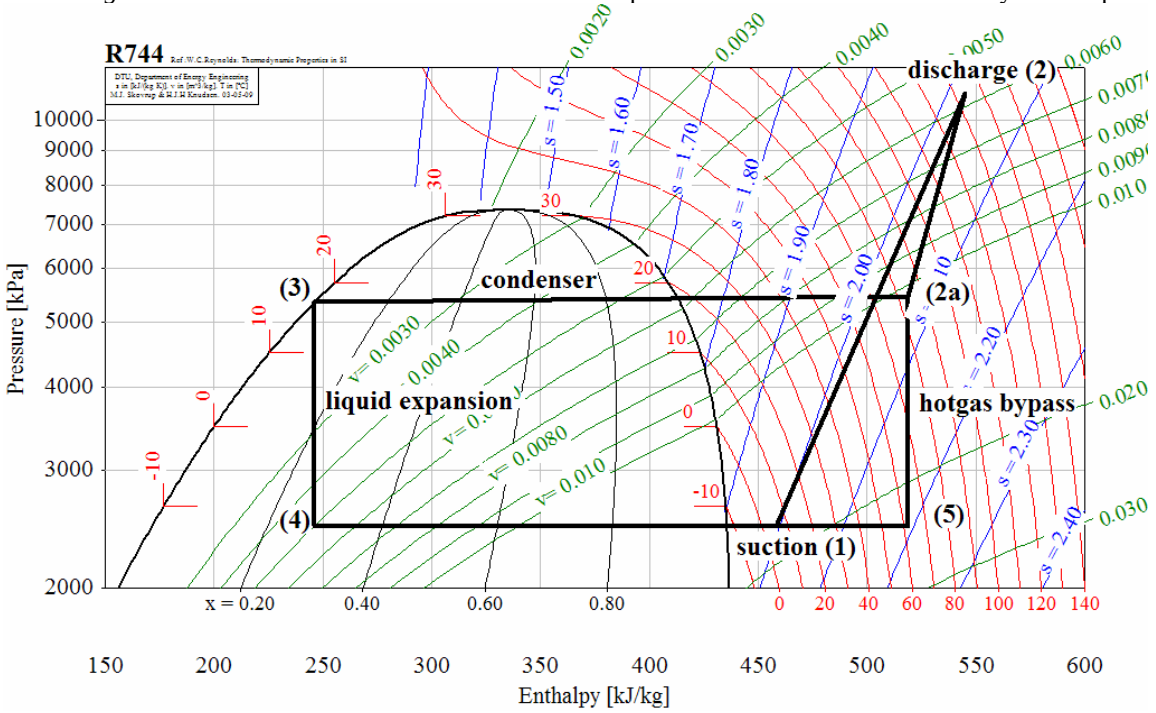

Figure 1*: Compressor load stand cycle in P-h-diagram*

The refrigerant oil is removed from the refrigerant by the oil-separator and returned to the suction line or compressor oil port. The oil-separator is extended with an oil-gauge, which contains a large sight glass to observe the oil level. During normal steady state operation, a constant oil level is maintained in the sight glass using a fine metering valve. In order to measure the oil volume flow rate, a shut-off valve, located downstream of the oil-gauge, is closed and the separated oil is collected in the oil-gauge for a certain time. The measurement of the collected oil together with the

time duration is used to determine the oil volume flow rate. Advantages of this setup are simplicity and permanent observation of the lubricant level. The method has an estimated measurement error of ±15 %.

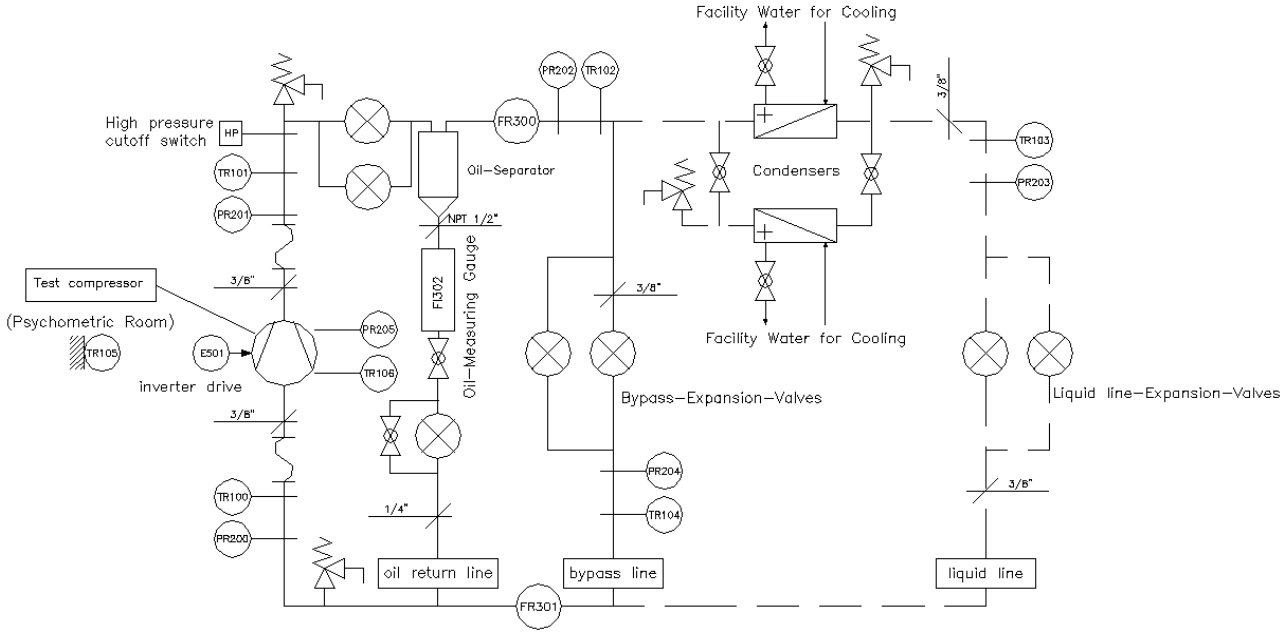

Figure 2: Load stand schematic with instrumentation

The load stand is equipped with Thermocouples (±1 K) to measure temperature and pressure transducers (±0.25 %) to measure the pressure at all five state points indicated in Figure 2. The refrigerant mass flow is determined by a Coriolis-based mass flow meter (±0.5 %) directly after the oil-separator (FR300). All of the sensors are connected to a data acquisition system, which records the measurements in 5-second intervals.

4. RESULTS

4.1 Compressor Specifications

Five prototype compressors were tested as part of the study presented here. The five compressors differ in type and design. This has some influence on the performances presented herein. Furthermore, the cooling capacities of the compressors range from 0.8 to 10.5 kW. However, the compressor's efficiency-characteristics can be compared regardless. The specifications of the compressors are listed in *Table 1*.

Table 1: Overview of compressor specifications

	Type A	Type B	Type C	Type D	Type E
Configuration	semi-hermetic	Hermetic	semi-hermetic	semi-hermetic	semi-hermetic
Type	reciprocating	rotary	reciprocating	reciprocating	reciprocating
Stages	1	2 (test without intercooling)	2 (test with intercooling)	1	1
Cylinders	2	2	2	1	1
Displacement	2 x 20.9 cm^3	3.33 cm^3/1.88 cm^3	28.8 cm^3/ 17.1 cm^3	2.45 cm^3	4.18 cm^3
Est. Cooling Cap.	8.3 kW	2.4 kW	10.5 kW	0.8 kW	1.6 kW
Shaft Speed	1740 rpm	4800 rpm	3588 rpm	3000 rpm	3525 rpm
Motor	3 x 480 V/60 Hz	DC-brushless	3 x 240 V/60 Hz	3 x 220 V/50 Hz	1 x 220 V/ 60Hz
Lubrication Oil	AN 32cSt	PAG 100cSt	PAG/AN 68 cSt	POE 85 cSt	PAG/AN 68 cSt

4.2 Operating Conditions

The operating conditions of the five compressors are summarized in *Table 2*. This table contains the compressor data that were taken at constant superheat. It can be seen from the table that the superheat values slightly differ for the five compressors. Nevertheless, the superheat variation has a rather small impact on the volumetric and overall isentropic efficiencies (Hubacher *et al.*, 2002 and 2003). Contrarily, a higher superheat has almost a direct impact on the discharge temperature. The superheat variation listed in *Table 2* is at the maximum 4 K. This indicates an acceptable deviation to directly compare the discharge temperatures of the compressors due to the fact that the discharge temperatures are at a level from 80 to 160 °C. Compressor D was tested at a different test matrix. The test matrix contained four blocks, each having four measurements with similar superheats. The superheat variation ranged from 20 to 50 K. Using only four data points with the same degree of superheat was not enough to curve-fit a second order polynomial for further evaluation. Compressor E contained tests with a superheat of up to 56K. Therefore, the obtained data from compressor D and E was corrected accordingly so that all of the data points refer to a superheat of 11 K. The refrigerant mass flow rate was corrected according to the model by Groll (2005) using a recommended correction factor F_1 of 0.75:

$$\frac{\dot{m}_{R,corr}}{\dot{m}_R} = 1 + F_1 \cdot \left(\frac{\rho_{1,corr}}{\rho_1} - 1 \right) \tag{1}$$

The correction factor F_1 was confirmed by analyzing compressor B where a correction factor F_1 of 0.79 was found. In a next step, the input power to the compressor was corrected according to the approach presented by Groll (2005):

$$\frac{\dot{W}_{comp,corr}}{\dot{W}_{comp}} = \frac{\dot{m}_{R,corr}}{\dot{m}_R} \cdot \frac{(h_{2s} - h_1)_{corr}}{(h_{2s} - h_1)} \tag{2}$$

Based on the results from Equation (1) and (2), all of the relevant performance indicators such as the volumetric and overall isentropic efficiencies were determined. In a last step, the discharge temperature was corrected based on a similar approach as given in Equation (1):

$$\frac{T_{2,corr}}{T_2} = 1 + F_2 \cdot \left(\frac{\rho_{1,corr}}{\rho_1} - 1 \right) \tag{3}$$

The correction factor F_2 was set to -1.3 based on the analysis of compressor B. Equation (3) and the obtained correction factor are subject to a certain inaccuracy. However, the tendency of this correction is correct. Furthermore, it was focus of this analysis to have a set of data at constant superheats in order to obtain second order polynomials of the performance indices. These polynomials were then used to evaluate the current status of the performance characteristic of CO_2-prototype compressors.

Table 2: Overview of operating conditions and errors

Compressor	Type A	Type B	Type C	Type D	Type E
Suction Pressure [MPa]	1.79 – 4.83	1.76 – 4.81	1.79 – 4.23	1.96 – 4.52	1.78 – 4.24
Discharge Pressure [MPa]	6.87 – 13.89	6.88 – 12.40	9.98 – 13.05	7.91 – 11.07	7.93 – 12.97
Pressure Ratio [-]	1.4 – 6.5	1.43 – 4.70	2.37 – 5.66	1.96 – 5.60	2.45 – 6.06
Superheat [°C]	10.7 ±2.3	14.6 ±2.3	11.5 ±0.4	11.0 ±0.0[*]	11.0 ±0.0[†]
Number of Data Points [-]	29	21	21	16	16
Error of Discharge Temperature [°C]	± 1.0	± 1.0	± 1.0	± 1.0	± 1.0
Average Error of Volumetric Eff. [%]	1.5	1.4	1.3	1.4	1.3
Average Error of Overall Isentropic Eff. [%]	6.2	6.4	4.6	4.8	6.5

[*] The performance of compressor type D was measured in test series of four similar degrees of superheating and thus, the obtained data was corrected to reflect a standard superheat of 11 K.

[†] The performance of compressor type E was measured with superheat up to 56K and thus, the obtained data was corrected to reflect a standard superheat of 11K

4.3 Approach and Analysis

The compressor performances were analyzed mainly on three aspects: the volumetric efficiency, the overall isentropic efficiency, and the discharge temperature. These parameters were evaluated for each completed steady-state test point. The discharge temperature was directly available from the measured data without further treatment. The volumetric efficiency was determined using equation (4), where the theoretical volume flow was obtained based on speed measurements and the displacement volume:

$$\eta_{vol} = \frac{\dot{m}_R \cdot v_1}{\dot{V}_{th}} \tag{4}$$

The overall isentropic efficiency is a frequently used measure for the first law efficiency of compressors by using an overall control volume, i.e., an evaluation by using the thermodynamic states at the compressor inlet and outlet. The overall isentropic efficiency is obtained based on equation (5):

$$\eta_{is,o} = \frac{\dot{m}_R \cdot (h_{2s} - h_1)}{\dot{W}_{comp}} \tag{5}$$

Once the discharge temperatures, the volumetric efficiencies, and the overall isentropic efficiencies were known for all operating conditions and each compressor, a suitable way to compare the performance parameters had to be found.

It is in the nature of compressor testing that it is impossible to test each compressor at exactly the same test matrix, which means that the operating conditions of each compressor differ in the suction and discharge pressure ranges. Thus, it is quite difficult to directly compare performance data for all four compressors. The authors have chosen an approach where they established compressor performance maps for each compressor using a second order polynomial without cross terms as given in Equations (6) to (8).

$$\eta_{vol} = a_0 + a_1 \cdot P_1 + a_2 \cdot P_1^2 + a_3 \cdot P_2 + a_4 \cdot P_2^2 \tag{6}$$

$$\eta_{is,o} = b_0 + b_1 \cdot P_1 + b_2 \cdot P_1^2 + b_3 \cdot P_2 + b_4 \cdot P_2^2 \tag{7}$$

$$T_2 = c_0 + c_1 \cdot P_1 + c_2 \cdot P_1^2 + c_3 \cdot P_2 + c_4 \cdot P_2^2 \tag{8}$$

The relatively simple compressor performance model deviates from the ANSI/ARI Standard 540-1999, which proposes a third order polynomial with cross-terms. In fact, the simpler second order model works with only 5 instead of 10 determination coefficients. *Table 2* lists the available number of data points for each compressor (16 to 29 data points). Based on this fact, at least 3 and at the maximum 6 data points determine one fitting coefficient. The second order model represents the compressor performance data quite well with RMS-errors for the discharge temperature in the range of ±1.2 to ±4.7 K. The RMS-mapping error for the volumetric efficiency ranges from 0.006 to 0.010 whereas the error range for the overall isentropic efficiency is between 0.008 and 0.016 (see Table 3 for more details). The authors share the standpoint that the above errors caused by the mapping are acceptable since this study presents the overall picture of the performance of carbon dioxide compressors rather than high accuracy compressor maps.

Table 3: RMS-Error as a measure of the goodness of the 2nd order polynomial fitting

RMS-Error	Type A	Type B	Type C	Type D	Type E
Discharge temperature	± 1.2 K	± 1.3 K	± 2.8 K	± 4.2 K	± 4.7 K
Volumetric efficiency	± 0.0092	± 0.0063	± 0.0063	± 0.0103	± 0.0104
Overall isentropic efficiency	± 0.0094	± 0.0095	± 0.0076	± 0.0155	± 0.0094

Figure 3 presents the superposition of the five tested pressure fields and indicates a common suction pressure range from 2 to 4 MPa. Therefore, the compressor performance data is plotted for suction pressures of 2, 3, and 4 MPa. Furthermore, it can be seen from the figure that the common discharge pressure range is only from 10 to 11 MPa. This is not very representative and thus, a discharge pressure range from 7 to 13.5 MPa was chosen for the compressor types A and B. The compressor performance of type C and D are represented on a discharge pressure range from 10 to 13.5 MPa and from 8 to 11.5 MPa, respectively. The compressor performance of type E is represented on a discharge pressure range from 8 to 13 MPa. Using the above definitions, the compressor performance charts were established for similar boundary conditions and individual pressure ratio ranges.

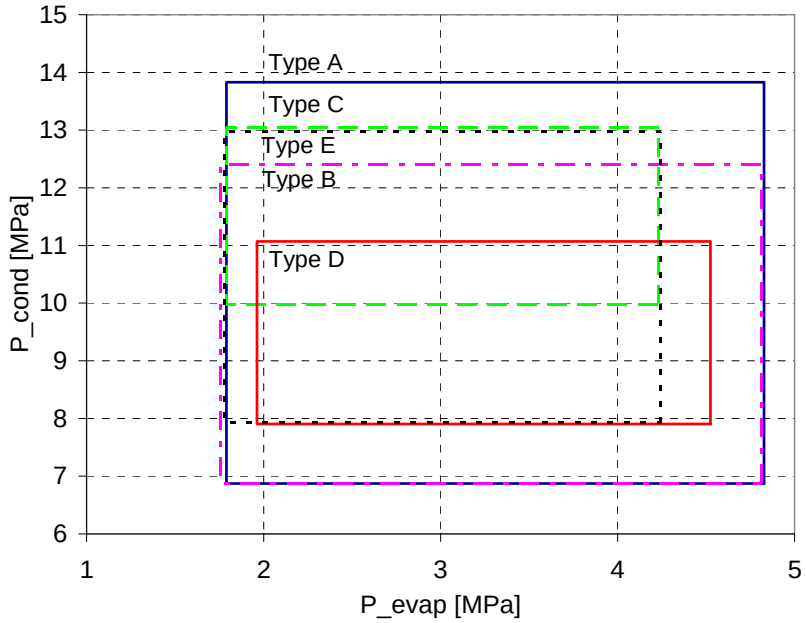

Figure 3: Superpositioning of all tested pressure fields of compressors A to E

4.4 Comparison of the Compressor Performances

The volumetric efficiency, the overall isentropic efficiency, and the discharge temperature of the five compressors A to E are presented in *Figure 4* to *Figure 6* as a function of the pressure ratio. Each diagram contains curves of the particular performance parameters as a function of suction pressures of 2, 3, and 4 MPa. The performances of the five compressors are superimposed on one diagram. Furthermore, square symbols represent data curves based on a suction pressure of 2 MPa, triangle symbols represent data curves for 3 MPa, and diamond symbols represent data points for 4 MPa, respectively.

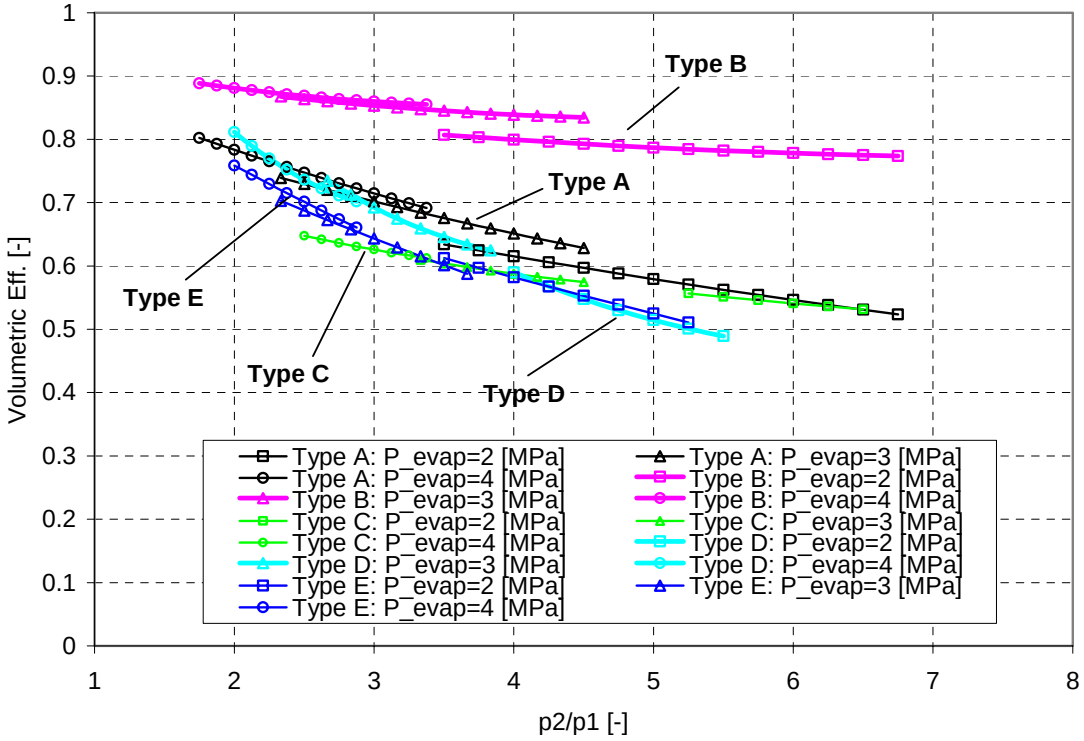

Figure 4: Volumetric efficiency for evaporation pressures of 2, 3, and 4 MPa versus pressure ratio

The volumetric efficiency is plotted in *Figure 4*. The figure indicates that compressor type A (rotary/hermetic) has the highest values between 0.78 and 0.9. The volumetric efficiencies of the other four compressors show similar characteristics. The values range from 0.5 to 0.8. The volumetric efficiency is associated with a total error (including fitting inaccuracy) from 1 to 11 % depending on the compressor type.

The overall isentropic efficiency is presented in *Figure 5*. The overall isentropic efficiency is the highest for the compressor type A at values from 0.63 to 0.73. In all cases, the overall isentropic efficiency increases with increasing suction pressures. For compressor types B, C, D and E most of the values are around 0.5. The compressor types A and B show a characteristic where the overall isentropic efficiency drops towards lower and higher pressure ratios. This is not the case for compressor C, D and E. While the overall isentropic efficiency from compressor C tends to increase towards higher pressure ratios it falls for compressor D and E. In general, the overall isentropic efficiency is relatively stable over a large pressure ratio range. The total uncertainty of the overall isentropic efficiency ranges between 5 and 20 % (including curve fitting error).

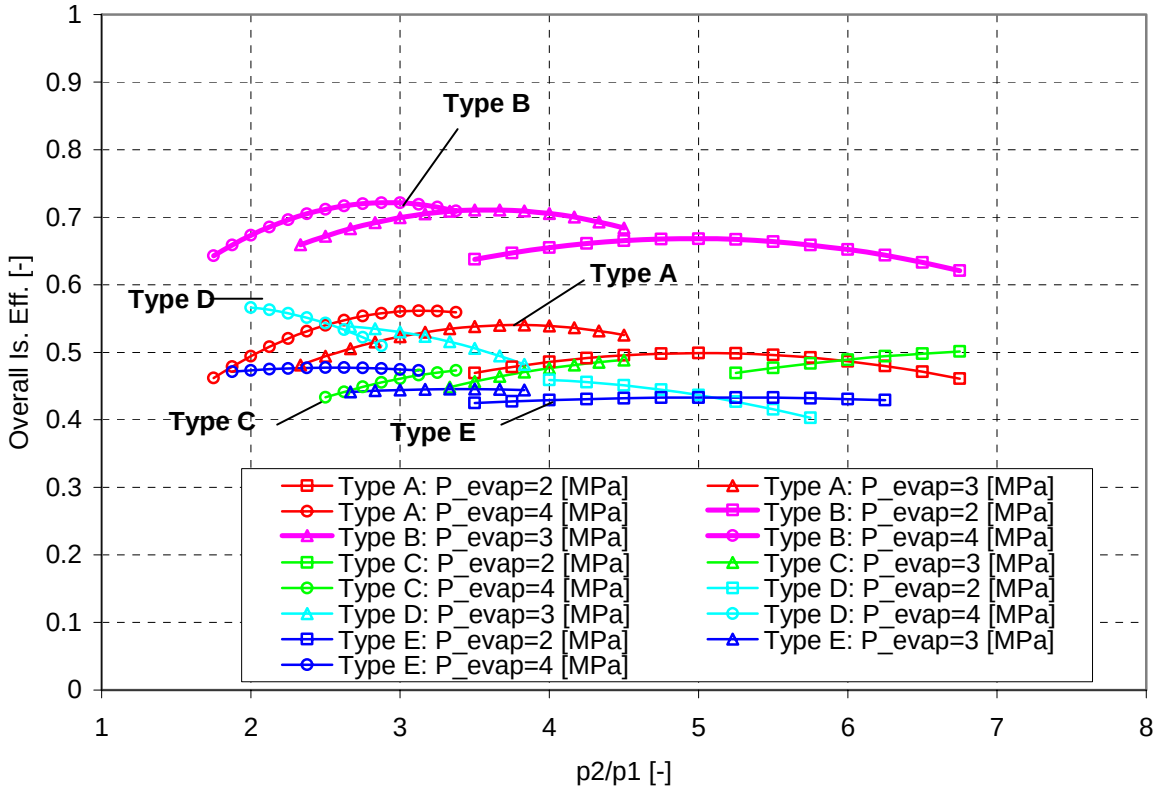

Figure 5: Overall isentropic efficiency for evaporation pressures of 2, 3, and 4 MPa versus pressure ratio

The third performance parameter of interest is the discharge temperature. Especially supercritical discharging of carbon dioxide can be associated with high temperatures. Therefore, it is important to know the discharge temperature range of prototype carbon dioxide compressors as studied in this paper. A large superheat directly impacts the discharge temperature towards higher values. However, it is usually the objective to keep the superheat relatively low. Therefore, a superheat of 10 to 15 K was chosen for the compressor performance evaluation. Furthermore, the influence due to the variation of the superheat is almost negligible with respect to the volumetric efficiency and the overall isentropic efficiency, while it is not for the discharge temperature. The superheats of the five compressors are outlined in *Table 2*. As mentioned before, the data of compressor type D and E were corrected to obtain compressor data at a superheat of 11 K. A variation of the superheat from 10 to 15 K only slightly impacts the discharge temperature. The discharge temperatures are presented in *Figure 6*. As expected, the discharge temperatures are highest for the lowest suction pressures. Also, the temperatures are quite close together and show similar characteristics. Overall, the discharge temperature ranges from 65 to 165 °C for pressure ratios from 2 to 7 whereas the largest increases are due to the pressure ratio changes. In terms of the different compressor designs, it can be seen that the intercooled two-stage compressor (type C) achieves no significant reduction in discharge temperature compared to the other compressor types. In addition, the compressor type B with a two-stage configuration and no intercool-

ing shows the highest discharge temperatures. This is surprising since the overall efficiency of this particular compressor is the highest and therefore, less input power is converted into irreversibilites. The associated discharge temperature error ranges between 1.2 and 4.8 K (including curve-fitting error) whereas the error of compressor D and E can be higher due to the superheat correction (see Section 4.2 "Operating Conditions").

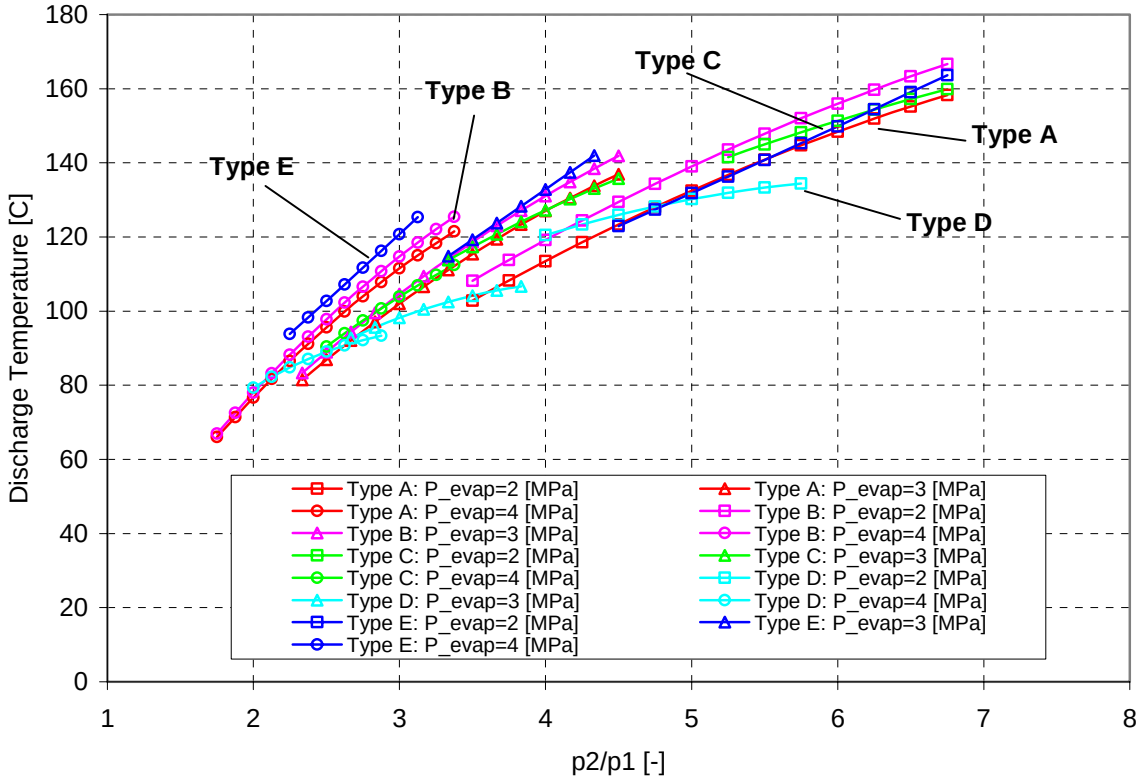

Figure 6: Discharge temperature for evaporation pressures of 2, 3, and 4 MPa versus pressure ratio

4.5 Data Reliability‡

In order to guarantee a high level of confidence in the compressor data and also to see the degradation of the compressor performance over the test time, the repeatability of the measurements at a standard test point was introduced. This test point was evenly distributed over the entire test matrix. The standard test had two purposes: on one hand, it was a performance monitoring tool, which eventually would have revealed performance dropping due to damage and on the other hand supplies a data population to determine the repeatability. It is obtained by using statistical methods such as the confidence interval (significance level of 0.01). The repeatability is then defined as:

$$R = \left(1 - \frac{Conf}{mean}\right) \cdot 100\ \% \tag{9}$$

Table 4 lists the individual repeatability levels for the different performance parameters and the four compressors. The second row lists the number of repetition tests, which were available for the repeatability analysis. It can be noted that the confidence in the measurements is very high for two reasons: First, high accuracy measurement devices were utilized in the load stand and second, the repeatability of the measurements is very high at 97.1 %.

Only manually operated needle valves were available at the time when the load stand was build and thus, the operation of the load stand is based on intensive hand work. However, once steady state is reached, the system operates very stable at most operating points without any fluctuations caused by a controller. It can also be noted that the basis for reliable and confident measurement data is sufficient time to reach a defined steady state operating conditions (30 minutes to one hour) and then a data collection of at least 30 minutes.

‡ No Repeatability of data points for Compressor Type E

Table 4: Repeatability of data points

Repeatability of:	Type A	Type B	Type C	Type D
# of repetition tests	7	7	2	2 x 2
Vol. efficiency	98.8%	99.8%	93.0%	94.7%
Ov. Isentropic eff.	99.4%	99.5%	98.8%	93.6%
Discharge Temperature	97.5%	99.3%	99.8%	91.1%
Overall average	97.1%			

4.6 Oil flow rate and mass flow measurement

As already stated earlier, the mass-flow measurement of the carbon dioxide was carried out using a Coriolis type mass-flow-meter at intermediate pressure after the oil separator and a volume-flow-meter in the suction line. Additionally, the compressor mass flow rate was verified during the compressor tests using an intercooler by applying an energy balance across the intercooler. All of these results were within a deviation of less than 2%.

To prove the efficient separation of the oil from the refrigerant, several tests were conducted to measure the oil-concentration in the carbon dioxide flow rate that leaves the oil-separator. The procedure described in ASHRAE-standard 41.4-1984R (1984) was applied. This standard uses an evacuated gas-cylinder which is connected to the liquid-line and filled with approximately 400 g of refrigerant-oil-mixture. After disconnecting the cylinder, the carbon dioxide is slowly released so that only the lubricant remains in the cylinder. By comparing the weight of the cylinder before and after this measure, the amount of oil in the refrigerant can be determined. These measurements were carried out both for compressors A and B for 3 samples each. The oil concentration for compressor A after the oil separator was 0.15% (±0.03%) and 0.33% (±0.03%) for compressor B.

The general approach for oil flow measurement was already presented in Section 3 of this paper. Table 5 presents the results of these measurements. For all reciprocating compressors the oil flow rate was relatively low with less than 1%. Only the rotary compressor shows an oil flow rate of up to 14% which is very disadvantageous in a real application and requires the use of an oil separator.

Table 5: Measured oil flow-rate for the compressors

Compressor	Type A	Type B	Type C	Type D	Type E
Oil Flow Rate	0.5 – 0.8 %	10 – 14 %	0.2 – 1.0 %	0.1 – 0.2 %	0.1 – 0.2 %

5. CONCLUSIONS

The transcritical carbon dioxide technology is an interesting and promising option for future refrigeration whereby new and efficient carbon dioxide compressors will be needed. This paper studied and compared the performance of five prototype carbon dioxide compressors, which were tested on an especially built carbon dioxide compressor load stand. This paper studied one rotary and four reciprocating compressors. Only the rotary compressor was hermetic, while the reciprocating compressors were configured as semi-hermetic compressors. Furthermore, two compressors (the rotary and one reciprocating) have two-stages and the two-stage reciprocating compressor was run with intercooling. The five compressors cover a cooling capacity range from 0.8 to 10.5 kW.

The compressor performance data was studied and compared for the most compressor-relevant parameters such as the volumetric efficiency, the overall isentropic efficiency, and the discharge temperature. In order to better compare the different data sets, compressor performance maps were established by using a second order polynomial curve-fitting approach. Then, the data was compared at similar suction pressure levels of 2, 3, and 4 MPa. The discharge pressure was varied within the individual limits in order not to exceed the sample data range. This leads to a pressure ratio range from approximately 2 to 7. Finally, the obtained performance data based on the compressor performance maps were superimposed for all compressors in one diagram each for volumetric efficiency, overall isentropic efficiency, and discharge temperature. The associated performance data uncertainties range between 2 and 7 %.

It was found that the gross overall isentropic efficiency ranges between 0.5 and 0.8 whereby values of up to 0.9 exist. The overall isentropic efficiency is less impacted by the pressure ratio and ranges from a main value of 0.5 to the highest value of 0.72, which was measured for the rotary compressor. Furthermore, the overall isentropic efficiency increases with suction pressures. The same can be said about the volumetric efficiency. Finally, the discharge temperature was compared. The five compressors show discharge temperature ranges from 65 to 165 °C whereby the latter temperature is reached for pressure ratios towards 7. As expected, the discharge temperatures are higher towards lower suction pressures. It can be noted that the discharge temperatures are relatively close together and the temperature increase towards higher pressure ratios follows the same trend.

6. REFERENCES

Adolph, U., "Einsatz von CO_2 als Kaeltemittel in Schienenfahrzeugen," FKW Seminar XVII, FKW GmbH, Hannover, Germany, Dec. 6, 1995.

Groll, E.A., "Analysis of Thermal Systems - Lecture 7: Compressors," Class Notes of ME 518, Purdue University, West Lafayette, IN, 2005.

Groll, E.A., "Recent Advances in the Transcritical CO_2 Cycle Technology," 18th National & 7th ISHMT-ASME Heat and Mass Transfer Conference, IIT Guwahati, India, January 4 - 6, 2006.

Fagerli, B.E., "CO_2 Compressor Development," Proc. IEA Heat Pump Centre/IIR Workshop on CO_2 Technology in Refrigeration, Heat Pump & Air Conditioning Systems, Trondheim, Norway, May 13-14, 1997.

Fagerli, B.E., "An Investigation of Possibilities for CO_2 Compression in a Hermetic Compressor," Proc. IIR Conf., Applications for Natural Refrigerants, Aarhus, Denmark, Sept. 3-6, pp. 639-649, 1996.

Fagerli, B.E., "Development and Experiences with a Hermetic CO_2 Compressor," Proc. 1996 Int. Compressor Eng. Conf. at Purdue, West Lafayette, IN, July 23-26, pp. 229-235, 1996.

Koehler, J., Sonnekalb, M., and H. Kaiser, "A Transcritical Ref. Cycle with CO_2 for Bus Air Conditioning and Transport Ref.," Proc. 1998 Int'l Ref. Conf. at Purdue, West Lafayette, IN, July 14-17, pp. 121-126, 1998

Koehler, J., Kaiser, H., and B. Lauterbach, "CO_2 as Refrigerant for Bus Air Conditioning and Transport Refrigeration," Proc. IEA Heat Pump Centre/IIR Workshop on CO_2 Technology in Refrigeration, Heat Pump & Air Conditioning Systems, Trondheim, Norway, May 13-14, 1997

Hubacher, B, Groll, E. A., and Hoffinger, C., "Performance Measurement of a Semi-Hermetic Carbon Dioxide Compressor", Proc. Int'l Refrig. Conf. at Purdue, West Lafayette, IN, July 16-19, pp. 477-485, 2002.

Hubacher, B., Groll, E. A., "Performance Measurement of a Hermetic, Two-Stage Carbon Dioxide Compressor", Proc. Int'l Conf. of Refrig. (IIR), Washington D.C., MA, August 17-22, 2003.

Hwang, Y., and R. Radermacher, "Development of Hermetic Carbon Dioxide Compressor," Proc. 1998 Int'l Refrigeration Conf. at Purdue, West Lafayette, IN, July 14-17, pp. 171-176, 1998.

Neksa, P., Dorin, F., Rekstad, M., and A. Bredesen, "Development of Two-Stage Semi-Hermetic CO2-Compressors" Proc. of the 4th IIR–Gustav Lorentzen Conference on Natural Working Fluids, Purdue University, West Lafayette, IN, July 25-28, pp. 355-362, 2000.

Tadano, M., Ebara, T., Oda, A., Susai, T., Takizawa, K., Izaki, H., and T. Komatsubara, "Development of the CO_2 Hermetic Compressor", *Proc. of the 4th IIR–Gustav Lorentzen Conference on Natural Working Fluids*, Purdue University, West Lafayette, IN, July 25-28, pp. 323-330, 2000.

7. NOMENCLATURE

Symbols:			Indices:	
h	Enthalpy	[kJ/kg]	1	State point 1 (compressor suction)
$\dot{m}$	Mass flow rate	[kg/s]	2	State point 2 (compressor discharge)
$\dot{W}$	Electrical power	[W]	corr	Corrected value
P	Pressure	[MPa]	R	Refrigerant
$\dot{V}$	Volume flow rate	[m^3/s]	s	Isentropic process
v	Specific volume	[m^3/kg]	comp	Compressor
ρ	Ref. density	[kg/m^3]		
F	Correction factor	[-]		
T	Temperature	[-]		
N	Number of data points	[-]		